AIAA 2013-4274

Wheels-Off Time Estimation at Non-ASDE-X Equipped Airports

Gano B. Chatterji* and Yun Zheng†
University of California Santa Cruz, Moffett Field, CA, 94035-1000

This paper is devoted to the development and evaluation of wheels-off time estimation and selection of airports without advanced automation that could benefit from wheels-off time estimation. After eliminating non-hub, small-hub, and airports with Airport Surface Detection Equipment Model-X, 29 airports were selected for further analysis. Using taxi-out delay, traffic management initiative delay counts and commercial operation counts as metrics in a multiple-metric K-Means method, these airports were organized into three groups. San Jose International, Cleveland-Hopkins International and San Francisco International are recommended for development and testing of wheels-off time estimation methods as they are suitable representatives of these three groups. The second part of the paper is devoted to wheels-off time estimation using a simulation procedure that uses kinematic models of different types of aircraft and a node-link graph to simulate surface traffic. The central idea is to integrate the aircraft equations of motion along the path in the node-link graph while complying with separation constraints and rules for waiting to cross intersections and active runways. While the intent was to apply the wheels-off estimation method to San Jose, the geometry data and the surveillance data were not received in time for this study. Therefore, modeling, simulation and tests were done with Dallas-Fort Worth traffic for which the needed data were available. Of the two approaches described in the paper, the data-driven approach, which uses historical taxi-times, can be readily applied to airports like San Jose, Cleveland and San Francisco.

I. Introduction

This paper is motivated by the need for predicting wheels-off time at airports where advanced automation systems, such as the Surface Decision Support System (SDSS), that depend on surveillance information derived from Airport Surface Detection Equipment Model-X (ASDE-X) type systems will not be available. At airports with SDSS type systems, aircraft surface movement will be scheduled, which will reduce runway entry time and wheels-off time uncertainty. Additionally, it will be possible to generate better estimates by using surveillance information. For example, the taxiway entry time of an aircraft waiting at the spot can be predicted more accurately by predicting the trajectories of aircraft in the movement areas starting from the current locations from surveillance data. At less equipped airports, wheels-off time will have to be estimated under the current day conditions with uncertainties associated with aircraft movement in the ramp-area and in the movement-area. Wheels-off time predictions are needed for coordinating departure release times with downstream facilities to meet flow management restrictions imposed by them. These restrictions are imposed for ensuring adequate separation between aircraft, creating orderly flows in terminal areas, and protecting sectors and airports from being overwhelmed by demand. Two of the commonly used restrictions that could benefit from wheels-off time estimation are Call For Release (CFR) and Expect Departure Clearance Time (EDCT). Accuracy requirement for CFR is actual wheels-off time within two-minutes early to one-minute late window with respect to the estimated wheels-off time. The requirement for EDCT is plus-minus five minutes.

In the first part of the paper, the initial set of 77 major U. S. airports in the Aviation System Performance Metrics (ASPM) database is reduced to the set of 29 airports after eliminating ASDE-X, small-hub and non-hub airports. This reduced set contains 27 medium-hub airports and two large-hub airports. Nine of these airports are being considered for surface surveillance systems. Currently, single radar-based Low Cost Ground Surveillance (LCGS) is

* Senior Scientist and Task Manager, U. C. Santa Cruz, MS 210-8, Associate Fellow.
† Software Engineer, U. C. Santa Cruz, MS 210-8.

being tested at San Jose International airport. Eight other airports including San Francisco International and Cleveland-Hopkins International will receive Automatic Dependent Surveillance-Broadcast (ADS-B) based Airport Surface Surveillance Capability (ASSC). These 29 airports are classified into groups using a K-Means method. The number of groups are then reduced to three based on the group IDs derived from K-Means classification. Reference 1 describes a similar study in which 21 large-hub airports were analyzed to determine suitable candidates for testing of NASA's Spot and Runway Departure Advisor (SARDA), which is discussed in Ref. 2, based on taxi-out delays, passenger enplanements, total operations and cargo operations.

The second part of the paper is devoted to wheels-off time estimation. The earlier study in Ref. 3 examined wheels-off time estimation using a neural network with metrics derived from historical surface surveillance data and ASPM database. That study analyzed data from Dallas-Fort Worth and showed that gate to runway distance is the most significant factor for wheels-off prediction. Other significant factors were 1) average taxi-out delay in previous 15-minutes, 2) number of departures on surface at actual gate departure time, 3) average taxi-out delay of departures on same runway in previous 15-minutes, 4) average taxi-out delay of departures to the same fix in the previous 15-minutes, 5) wind angle and 6) airport arrival rate set by air traffic control. Results showed that wheels-off time could be predicted within two-minutes early to one-minute late window 59% of the time. In this paper, two approaches are described- a simulation-based approaches and a data-driven approach. The first method is purely model-based. Ramp-area and movement-area speeds are specified in the simulation. This method does not require surveillance information. The second method, data-driven method, uses gate and spot to queue-area, runway and wheels-off taxi -times derived from historical surveillance data to estimate queue-area and runway entry times and wheels-off time. Queue-area and runway entry times were estimated in addition to wheels-off time to determine loss of estimation accuracy in these regions of surface movement. The proposed methods assume that gate pushback time or spot crossing time and taxiway path of the flight specified by taxiway clearance are known. Aircraft position is obtained as a function of time by integrating the equations of motion along the specified path in the simulation-based method. Possible sources of errors in surface trajectory prediction are the differences in actual and assumed taxi-speed, surface winds and visibility, congestion caused by other aircraft, and takeoff and landing demand. Six days of August 2011 Dallas-Fort Worth surface data were processed to generate queue-area and runway entry times and wheels-off time using the two methods. These estimates were then compared against those derived by processing the actual surveillance data to determine temporal errors and entry sequence errors.

Section II describes the metrics and method for selection of non-ASDE-X airports. Section III describes the simulation-based method and the data-driven method for estimating queue-area entry time, runway entry time and wheels-off time. Queue-area entry time, runway entry time and wheels-off time errors, and sequence errors with respect to surveillance derived values are presented in Section IV. Conclusions and future work are discussed in Section V. A listing of the 77 ASPM airports is provided in the Appendix. Numerical values of the metrics used for selecting airports are also listed in a table in the Appendix.

II. Selection of Non-ASDE-X Airports

In this section, the sources of taxi-out delay, taxi-out time, number of commercial operations, traffic flow management initiative caused delay counts, passenger enplanement counts, type of hub airport and type of surface surveillance equipment at the airport used for determining the non-ASDE-X airports in this study are described. Most of the data were derived from the Federal Aviation Administration's (FAA) Aviation System Performance Metrics (ASPM) and Operations Network (OPSNET) databases containing historical traffic counts and delay statistics. Data were also derived from the Terminal Area Forecast (TAF) Summary for fiscal years 2011-2040 report. The 77 airports included in the ASPM and OPSNET databases are listed in Table A-1 in the Appendix. These airports are referred to by their airport code in the rest of the document.

The first report obtained from the ASPM database is the "Analysis By Airport Report (compared to flight plan)" for calendar year 2011. This report includes average taxi-out time and average taxi-out delay for each of the 77 major U. S. airports. Taxi-out time is the difference between the actual wheels-off time and the actual gate-out time. Taxi-out delay is difference between the taxi-out time and the unimpeded taxi-out time. Taxi-out times and delays are in minutes. Only data from itinerant flights to or from the ASPM 77 airports or operated by one of the ASPM 29 carriers are included. Itinerant flights are those that land at an airport, arriving from outside the airport area, or depart an airport and leave the airport area. Data on flights by ASPM carriers to international and domestic non-ASPM airports are also kept in the ASPM database. General aviation and military flights are excluded. Table A-2 in the Appendix lists the average taxi-out delay and the taxi-out delay ratio derived from this report. The average taxi-out delay ratio is defined as the ratio of average taxi-out delay to average taxi-out time.

The second report, "OPSNET: Airport Operations: Standard Report" for calendar year 2011 is obtained from the OPSNET database. This same report can also be obtained from the FAA's Air Traffic Activity System (ATADS) database. This report contains air-carrier, air-taxi, general aviation and military itinerant operations, and civil and military local operations. Local operations are performed by aircraft that remain in the local traffic pattern, execute simulated instrument approaches or low passes at the airport, and fly to or from the airport and a designated practice area within a 20−mile radius of the tower. Airport operations include all arrivals and departures at the airport; overflights are not included. OPSNET defines air-carrier as aircraft with a seating capacity of more than 60 seats or a maximum payload capacity of more than 18,000 pounds carrying passengers or cargo for hire or compensation and air-taxi as aircraft with a seating capacity of 60 or less or a maximum payload capacity of 18,000 pounds carrying passengers or cargo for hire or compensation. Air-carrier includes U. S. and foreign flagged carriers. Table A-2 in the Appendix lists the sum of itinerant air-carrier and air-taxi operations (commercial operations as defined by TAF report) for each of the 77 major U. S. airports based on the 2011 report.

The third report, "OPSNET: Delays: Delay Types Report" was obtained from OPSNET database to get TMI-from delay counts for calendar year 2011. These counts are also listed in Table A-2 in the Appendix. OPSNET defines TMI-from delays as traffic management initiative delays from a national or local traffic management initiative as experienced by aircraft departing from the selected facilities. These initiatives include departure spacing (DSP), enroute spacing (ESP), arrival spacing (ASP), miles-in-trail (MIT), minutes-in-trail (MINIT), Expect Departure Clearance Time (EDCT), Ground Stop (GS), and Severe Weather Avoidance Plan (SWAP). It should be understood that these delays are charged to facilities asking for the delays and not to the ones providing the delays. For example, 11,132 aircraft were delayed at Atlanta (see ATL TMI-from delay counts in Table A-2 in the Appendix) to comply with traffic management initiatives of other facilities. From this study's perspective, TMI-from delay counts (number of aircraft experiencing TMI-from delays) indicates instances when improved wheels-off time estimate at the departure airport could help meet metering and spacing constraints imposed by others.

The fourth report derived from OPSNET database, "OPSNET: Delays: EDCT/GS/TMI By Cause Report" provided the TMI-to weather delay counts and TMI-to volume delay counts. TMI-to delays is defined as delays resulting from a national or local traffic management initiative reported in OPSNET and charged to the facility that is the originating cause of the restriction. These initiatives also include DSP, ESP, ASP, MIT, MINIT, EDCT, GS, and SWAP. These delays may be experienced by aircraft at another facility, but are charged to the causal facility. For example, 5,561 aircraft were delayed at other airports due to weather caused restrictions imposed by Atlanta as listed in Table A-2 in the Appendix. TMI-to volume delays are caused by restrictions imposed for moderating the traffic demand. In addition to weather and volume delay counts and minutes, the report contains delays due to equipment, runway and other causes.

Passenger enplanements data listed in Table A-2 in the Appendix were obtained from the main FAA website in the "Passenger Boarding and All-Cargo Data" Section (see Ref. 4). The main source of enplanement statistics is the U. S. Department of Transportation (DOT). Scheduled and nonscheduled U. S. certificated air-carriers, commuter air-carriers, and small certificated air-carriers submit data to DOT on Form 41 Schedule T-100. Foreign flag air carriers submit data to DOT on Form 41 Schedule T-100(f). In addition, an annual survey of air-taxi/commercial operators, who report their nonscheduled activity on FAA Form 1800-31, is conducted by the FAA. As one would expect, passenger enplanement is highly correlated to the number of commercial operations. The value of the correlation coefficient (also known as Pearson's correlation coefficient and Pearson's product-moment correlation coefficient) was found to be 96.7% and the p-value was found to be zero to six decimal places, which indicates highly significant correlation. Figure 1 shows the plot of passenger enplanements as a function of commercial operations based on the data in Table A-2 in the Appendix. The dotted line indicates a linear fit between enplanements and commercial operations. The coefficient of determination (R^2 value) was found to be 0.935. A closer look at enplanement data and commercial operations data in Table A-2 in the Appendix indicates some data inconsistencies. For example, 3,634 air-carrier and air-taxi operations were conducted at Oxnard, CA (OXR), but the number of enplanements is just 3. Similarly, numbers look very low for GYY, TEB, and VNY. The

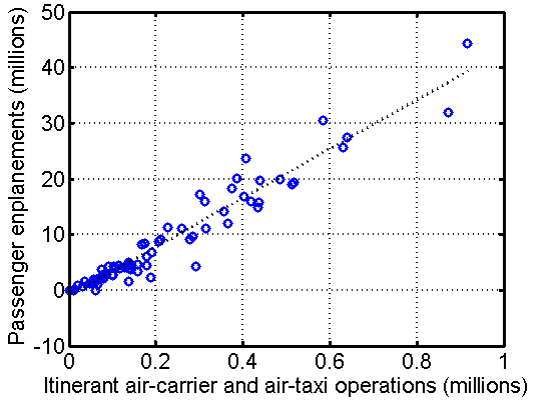

Figure 1. Correlation between commercial operations and passenger enplanements.

following response was received from the FAA when asked for an explanation for the discrepancy. The enplanement numbers posted by the FAA include all revenue passengers that boarded a flight conducted by a large certificated, commuter, or foreign air-carrier. They also include the enplanements for on demand air-taxi operators. However, these small operators are not required to report their passenger enplanements to the FAA. So while FAA has some data, it can vary from year to year based on whether the operators voluntarily report their passenger activity. This impacts the non-primary airports like TEB and VNY that serve corporate and business flights which may have a significant number of Part 135 on demand operations.

FAA facility pay level data listed in Table A-2 in the Appendix were obtained from the "OPSNET: Facility Information: Detail Report" derived from the OPSNET database. Reference 5 provides a complete description of the formula for pay setting. The facility pay level varies between "null" and 12. Null level is indicated by a zero in the table. Since facility pay level is based on a formula that considers both the number of operations and complexity factors such as, tower with or without radar, performance characteristics of aircraft using the airport, runway and taxiway layout, proximity to other airports, military operations and terrain, it can be used as a metric for categorizing airports. Correlation between the number of operations and the levels given in Table A-2 was found to be 68.6%. The correlation improved to 78% with 0 levels excluded. In both these instances, the correlations were determined to be significant with p-value of zero up to six decimal places. It is thus seen that number of operations dominates the formula for pay setting.

ASPM and OPSNET databases provide operational statistics on Core airports, Operational Evolution Partnership (OEP 35) airports, 45 airports tracked in OPSNET (OPSNET 45) and the 77 airports tracked in ASPM. Core airports are the 30 busiest commercial U. S. airports that serve as hubs for airline operations at major metropolitan areas. OEP 35 airports are commercial U.S. airports with significant activity. These airports serve major metropolitan areas and also serve as hubs for airline operations. More than 70 percent of passengers move through these airports. The Venn-diagram in Fig. 2 shows the airport codes of the Core, OEP 35, OPSNET 45 and ASPM 77 airports. The rectangular box shows all the 77 ASPM airports. The 30 Core airports are enclosed in the innermost circle with thick solid boundary. All the Core airports and five additional airports enclosed in the circle with dotted line boundary form the OEP 35 airport set. OPSNET 45 airports are enclosed in the largest circle with a thin solid boundary. Observe that OPSNET 45 set contains all the Core and OEP 35 airports except Honolulu International airport (HNL). The 31 airports outside the circles only belong to ASPM 77.

The airports in Fig. 2 were identified as large-hub airports, medium-hub airports, small-hub airports and non-hub airports based on their designation in Ref. 6. A large-hub airport is defined as an airport with 1% or more of total U. S. passenger enplanements. A medium-hub airport is defined as an airport with 0.25% to 0.99% of total U. S. passenger enplanements. An airport with 0.05% to 0.249% of total U. S. passenger enplanements is categorized as a small-hub airport. Finally, an airport with less than 0.05% of total U. S. passenger enplanements is termed a non-hub airport. All Core airports other than Memphis International airport (MEM) are large-hub airports. These 29 airport codes inside the smallest circle are shown in red without a superscript. The 34 medium-hub and 6 non-hub airports are indicated in black and magenta, and by "m", and "*" superscripts, respectively. The airport codes of 8 small-hub airports are in blue and underlined.

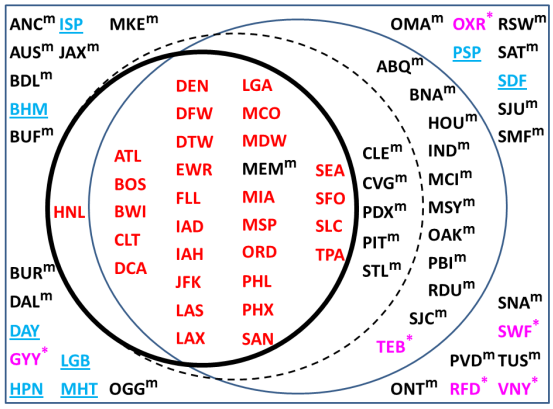

Figure 2. ASPM 77 airports categorized as large-hub, medium-hub, small-hub and non-hub airports.

Figure 3 shows the airport codes of ASDE-X airports, Low Cost Ground Surveillance (LCGS) airports and Airport Surface Surveillance Capability (ASSC) airports. List of names of airports with ASDE-X, LCGS and ASSC were obtained from Refs. 7-9. LCGS is based on single surface movement radar concept. FAA is currently evaluating LCGS at Spokane (GEG), Manchester (MHT), San Jose (SJC), Reno (RNO) and Long Beach (LGB). Airport codes of LCGS airports are indicated in blue with a "*" superscript. As opposed to ASDE-X that uses radar, multilateration and Automatic Dependent Surveillance-Broadcast (ADS-B), ASSC derives data from just multilateration and ADS-B. FAA expects ASSC to begin tracking transponder-equipped aircraft and ADS-B equipped ground vehicles by 2017 at Portland (PDX), Anchorage (ANC), Kansas City (MCI), New Orleans (MSY), Pittsburgh (PIT), San Francisco (SFO), Cincinnati (CVG), Cleveland (CLE) and Andrews Air Force Base. ASSC airport codes in green are underlined. Airports without a surface

surveillance system are indicated with airport codes in black with an "n" superscript. The remaining 35 airports in red are ASDE-X airports.

After removing all the ASDE-X airports, small-hub and non-hub airports from Fig. 3, the remaining 29 airports shown in Fig. 4 are considered as suitable candidates for further analysis. San Francisco and Tampa are the only two large-hub airports remaining in this set. The other 27 are medium-hub airports. Nine airports in this set will either have LCGS or ASSC systems for surface surveillance. Since surveillance data can be used for comparing estimates against reality, these airports could be considered for near term development and testing of wheels-off time estimation methods.

To identify airports that could benefit from wheels-off time estimation, the important metrics are, 1) taxi-out delay, 2) TMI-from delay counts and 3) number of commercial operations. Without a suitable means for accounting for taxiway delays due to interactions between arriving and departing aircraft, one could resort to estimating wheels-off time based on the single value of taxi-time for the airport from ASPM database. This however, would lead to larger wheels-off time prediction errors at airports with larger taxi-out delays. Thus, airports with larger taxi-out delays can be expected to benefit more by being able to reduce larger wheels-off time prediction errors by employing a wheels-off time estimation method. Airports with TMI-from delays have to ensure that the affected aircraft depart at times coordinated with downstream facilities so that the restrictions imposed by them are met. Airports with higher TMI-from delay counts have to depart more aircraft on time; therefore, wheels-off time estimate can be expected to have a greater impact at these airports. Finally, improved predictability of taxi-time and wheels-off time has the potential of improving planning and scheduling for greater surface movement efficiency at busier airports, the ones with large number of commercial operations.

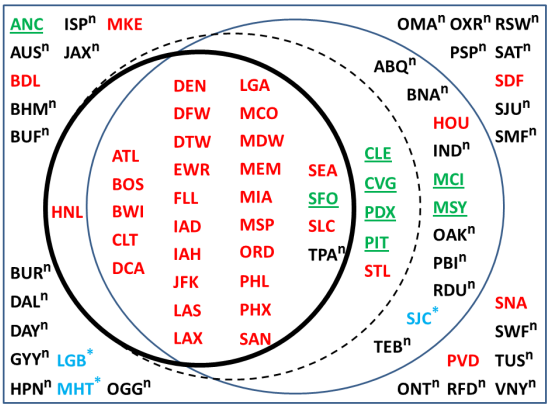

Figure 3. Airports with ASDE-X, LCGS and ASSC surface surveillance systems, and airports without surface surveillance systems.

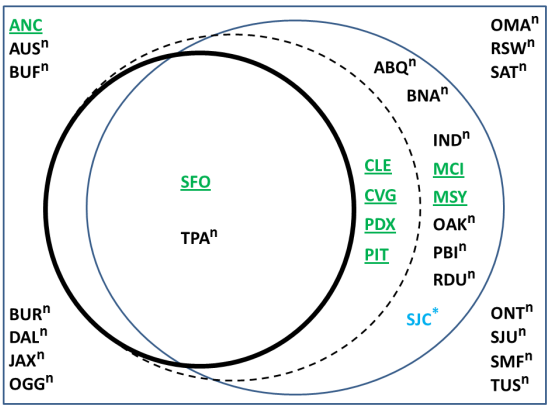

Figure 4. Airports remaining after removing ASDE-X airports, and small-hub and non-hub airports.

In addition to estimating taxi-out time, gate departure time needs to be known or estimated for wheels-off time prediction since wheels-off time is obtained by adding the taxi-out time to the gate departure time. Unfortunately, gate departure time is difficult to estimate. If airlines are unable to provide gate departure times prior to actual departure, the only choices are scheduled departure time from the Official Airline Guide (OAG) or proposed departure time from filed flight-plans. These times, however, are not accurate. It is also difficult to estimate gate departure delay by observing airport state data. The study in Ref. 3 found the correlation between gate departure delay and metrics derived from airport state data such as, number of aircraft on the surface, airport departure rate, wind and visibility to be quite low. Like Ref. 3, this study also assumes that gate departure time is known.

To group the 29 airports shown in Fig. 4 based on the values of taxi-out delay, TMI-from delay counts and number of commercial operations, and the other metrics listed in Table A-2 in the Appendix, the multiple-metric K-Means classifier described in Ref. 10 is used. The K-Means method partitions data into specified number of groups such that the means associated with the groups are as widely separated as possible. Data elements are then labeled based on their closeness to the group means for reducing the variance. Group means are then re-computed based on the elements assigned to the groups. The process of assignment of elements to the groups and computation of group means is continued till convergence is achieved, that is, group means do not change with successive iterations. The

three groups obtained based on taxi-out delay are summarized in Table 1. The minimum, mean, standard deviation and maximum values for each group are listed in the last four columns. Airport codes in each group are arranged in the non-increasing order. For example, ONT has the maximum taxi-out delay in Group 1 and OGG has the minimum taxi-out delay in Group 1. The three groups can be considered to be low, medium and high taxi-out delay groups. Groups obtained with TMI-from delay counts and with number of commercial operations are summarized in Tables 2 and 3. Observe from Table 2 that Raleigh-Durham (RDU) has to comply with more departure restrictions compared to the other airports. San Francisco (SFO), which has the most taxi-out delays and number of commercial operations, is a member of Group 2 in Table 2 with TMI-from delay counts of 1,848 in the year 2011 (see Table A-2 in the Appendix). Grouping based on taxi-out delay ratio and FAA level are summarized in Tables 4 and 5.

Table 1. Grouping based on average taxi-out delays in minutes.

Group ID	Airports	Min.	Mean	Std.	Max.
1	ONT, MSY, BUR, IND, AUS, SJU, CVG, SJC, OAK, DAL, ANC, OGG	1.5	1.9	0.2	2.1
2	RDU, PIT, CLE, SAT, TUS, ABQ, BNA, RSW, TPA, BUF, PBI, PDX, JAX, MCI, OMA, SMF	2.2	2.5	0.3	3.2
3	SFO	4.4	4.4	0.0	4.4

Table 2. Grouping based on TMI-from delay counts.

Group ID	Airports	Min.	Mean	Std.	Max.
1	MSY, PDX, AUS, SAT, OMA, DAL, SMF, BUR, SJC, OAK, TUS, ABQ, ONT, SJU, ANC, OGG	10	459	284	905
2	CVG, PIT, CLE, IND, SFO, BUF, TPA, MCI, BNA, PBI, JAX, RSW	1,172	1,772	412	2,531
3	RDU	3,557	3,557	0	3,557

Table 3. Grouping based on number of commercial operations.

Group ID	Airports	Min.	Mean	Std.	Max.
1	DAL, SAT, AUS, SJC, MSY, SMF, OGG, ABQ, BUF, PBI, OMA, JAX, ONT, RSW, BUR, TUS	57,648	90,430	18,572	116,414
2	PDX, ANC, CLE, TPA, CVG, RDU, BNA, IND, MCI, SJU, OAK, PIT	127,723	153,339	22,103	190,108
3	SFO	386,941	386,941	0	386,941

Table 4. Grouping based on average taxi-out delay ratio in percentage.

Group ID	Airports	Min.	Mean	Std.	Max.
1	AUS, OGG, IND, SJU, ANC, CVG	13.9	15.6	1.5	17.3
2	ONT, CLE, PIT, SMF, BNA, TPA, PDX, RSW, MSY, OAK, BUF, MCI, DAL, OMA, BUR, PBI, JAX, SJC	17.9	19.9	1.3	22.0
3	SFO, ABQ, SAT, RDU, TUS	23.3	24.2	1.5	26.8

Comparing Table 1 to Table 4, it is seen that ten airports (ONT, MSY, BUR, SJC, OAK, DAL RDU, SAT, TUS and ABQ) in Table 1 move one level higher in Table 4. These airports have higher average taxi-out delays compared to their nominal taxi-out times. Comparing Table 3 to Table 5, it is seen that 13 airports (ABQ, AUS, JAX, MSY, PBI, BUF, DAL, RSW, TUS, CVG, TPA, CLE and PIT) moved one level up in Table 5, one airport- SAT jumped

two levels higher, and only two airports- SJU and SFO moved one level down. This reconfirms the finding that the number of operations is significantly correlated to the FAA pay level. Thus, FAA pay levels can be used in lieu of number of commercial operations.

Finally, grouping based on TMI-to weather delay counts and TMI-to volume delay counts are given in Tables 6 and 7, respectively. Only airports that delayed at least 10 aircraft in the year 2011 were considered for grouping in Tables 6 and 7. This reduced the set of 29 airports to just 8 based on TMI-to weather delay counts. San Francisco, the sole member of Group 3 in Table 6, is known to be severely affected by visibility. In 2011, it was responsible for causing over 18,000 aircraft bound for SFO to be delayed elsewhere. Only three airports- CLE, SFO and DAL in Table 7 caused aircraft bound for those airports to be delayed elsewhere due to traffic volume. It is reasonable to

Table 5. Grouping based on FAA level.

Group ID	Airports	Min.	Mean	Std.	Max.
1	BUR, OGG, SJC, SJU, OMA, ONT, SMF	6	6.6	0.5	7
2	ABQ, AUS, BNA, IND, JAX, MCI, MSY, PBI, RDU, SFO, ANC, BUF, DAL, OAK, PDX, RSW, TUS	8	8.6	0.5	9
3	CVG, TPA, CLE, PIT, SAT	10	10.4	0.6	11

Table 6. Grouping based on TMI-to weather delay counts.

Group ID	Airports	Min.	Mean	Std.	Max.
1	CLE, IND, TPA, RDU, CVG, SAT	18	49	49	146
2	DAL	300	300	0	300
3	SFO	18,679	18,679	0	18,679

expect that departures would be affected when arrivals are impacted by weather and traffic volume. Wheels-off time estimates at these airports would have to consider weather and traffic volume conditions.

Table 7. Grouping based on TMI-to volume delay counts.

Group ID	Airports	Counts
1	CLE	11
2	SFO	24
3	DAL	173

The grouping results discussed above in Tables 1 through 7 considered a single metric for classification. Groups can also be formed by first creating a composite ID for each airport based on single metric classifications and then placing all the airports with the same ID in a group. For example, CVG is a member of Group 1 based on taxi-out delay, Group 2 based on TMI-from delays and Group 2 based on number of commercial operations, therefore its composite ID is (1, 2, 2). Similarly, the composite ID of IND is (1, 2, 2). Thus, CVG and IND belong to the same group based on their composite ID. This method is described in Ref. 10. Table 8 lists the airport grouping with composite ID constructed based on Tables 1, 2 and 3. Following this procedure, a member of group with Group ID (3, 3, 3) would be expected to benefit the most from wheels-off time estimation. Mean values of taxi-out delay, TMI-from delay counts and number of commercial operations for each group of airports are listed in the columns with headings- Mean 1, Mean 2 and Mean 3, respectively. Airport codes of airports that will receive ASSC for surface surveillance are shown in green boldface type and underlined. Airport code of San Jose, where LCGS is being tested, is shown in blue boldface type with "*" superscript. Table 8 shows that other than groups with IDs (2, 1, 1), (2, 2, 1) and (2, 3, 2), there is at least one airport in the group that will have a surveillance system. These airports should be initially targeted for developing and testing wheels-off time estimation methods. Track data (position as a function time) from surveillance can be used to determine gate, gate departure time, spot crossing time, ramp-area path and taxiway path needed for developing wheels-off time estimation methods. The estimated wheels-off time can be compared with the actual wheels-off time also using actual track data. The nine groups in Table 8 can be reduced further by merging smaller adjacent groups. Table 9 presents such a grouping by first giving preference to number of commercial operations and then to TMI-from delay counts using the Group IDs. The first group consisting of Group IDS (1, 1, 1), (2, 1, 1) and (2, 2, 1) has MSY and SJC, two airports that will have surface surveillance systems. The second group of airports consisting of Group IDs (1, 1, 2), (2, 1, 2), (1, 2, 2), (2, 2, 2) and (2, 3, 2) has six airports- ANC, PDX, CVG, CLE, MCI and PIT

that will receive ASSC. One of these airports can be chosen to represent the second set. The third group consisting of Group ID (3, 2, 3) has SFO as its sole member, an airport that will have ASSC. Thus, SJC with LCGS, CLE with ASSC and SFO with ASSC are good choices for representing the three groups in Table 9.

Table 8. Grouping based on taxi-out delay, TMI-from delay counts and number of commercial operations.

Group ID	Airports	Mean 1	Mean 2	Mean 3
1, 1, 1	AUS, OGG, BUR, DAL, MSY, ONT, SJC*	1.9	468	97,406
1, 1, 2	ANC, SJU, OAK	1.8	221	151,643
1, 2, 2	CVG, IND	2.0	2,209	149,239
2, 1, 1	OMA, SMF, ABQ, SAT, TUS	2.4	503	90,671
2, 1, 2	PDX	2.3	887	190,108
2, 2, 1	BUF, JAX, PBI, RSW	2.3	1,425	77,920
2, 2, 2	BNA, CLE, MCI, PIT, TPA	2.5	1,859	150,431
2, 3, 2	RDU	3.2	3,557	144,399
3, 2, 3	SFO	4.4	1,848	386,941

Table 9. Grouping based on preferences to number of commercial operations and TMI-from delay counts.

Group ID	Airports	Mean 1	Mean 2	Mean 3
1, 1, 1	AUS, OGG, BUR, DAL, MSY, ONT, SJC*	1.9	468	97,406
2, 1, 1	OMA, SMF, ABQ, SAT, TUS	2.4	503	90,671
2, 2, 1	BUF, JAX, PBI, RSW	2.3	1,425	77,920
1, 1, 2	ANC, SJU, OAK	1.8	221	151,643
2, 1, 2	PDX	2.3	887	190,108
1, 2, 2	CVG, IND	2	2,209	149,239
2, 2, 2	BNA, CLE, MCI, PIT, TPA	2.5	1,859	150,431
2, 3, 2	RDU	3.2	3,557	144,399
3, 2, 3	SFO	4.4	1,848	386,941

III. Wheels-off Time Estimation Method

In this section, the procedure for estimating wheel-off time at the 29 non-ASDE-X airports in Table 9 is described. It is assumed that airport geometry is available. Taxiways and runways are usually represented by polygons, where the locations of the vertices of polygons are specified by Cartesian coordinates with respect to a frame of reference. Locations of gates and spots are also specified with respect to the same frame of reference. Gate and spot locations and the polygons can be processed to create the node-link graph of the airport. An example of a node-link graph is shown in Fig. 5. Reference 11 describes the procedure for creating the node-link graph using taxiway and runway polygons. Any physical path for going from one location to another on the airport surface is represented by a sequence of nodes and links in this node-link graph. A location on the node-link graph is thus equivalent to a location on the physical airport surface. Since polygons, which are area elements, are represented by links, which are line elements, traversing along the links can be thought of as traversing along the taxiway centerline.

Given this node-link graph representation, the first step of the proposed wheels-off time prediction consists of representing the taxi clearance issued by the controller as a path in the node-link graph. Taxiway clearance is specified as an ordered list of taxiway segments that the aircraft is required to follow after pushback from the gate to runway. Mapping from taxiway segments to polygons and from polygons to links is used to determine the path in the node-link graph. In this early phase of development, aircraft position data acquired by ASDE-X during surface movement at Dallas-Fort Worth airport are derived from recorded SDSS logs to identify path from gate to runway in the node-link graph. Polygon containing the aircraft position is identified and then polygon to link mapping is used to identify the corresponding link. The sequence of links then determines the path.

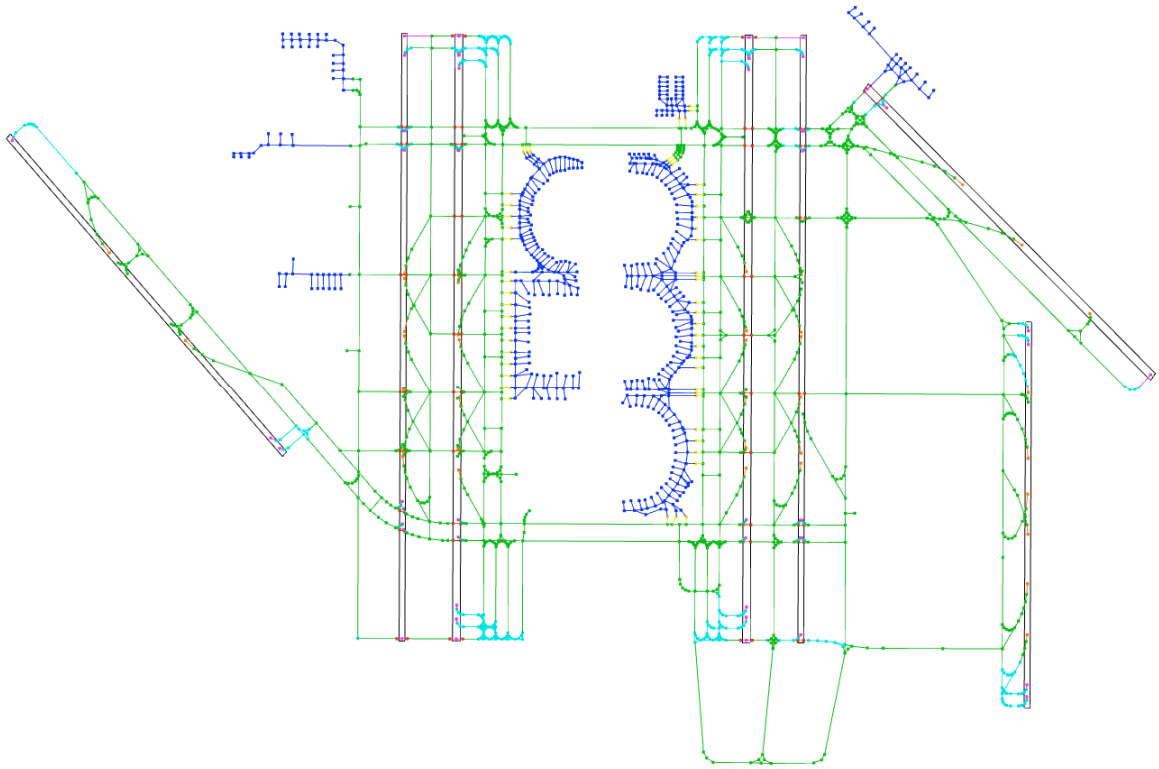

Figure 5. Node-link graph of Dalla-Fort Worth airport.

The next step of the wheels-off time prediction consists of integrating the aircraft equations of motion along the path in the node-link graph. Starting with the gate location and the gate pushback time, this process generates a time history of positions along the path. This is the classical procedure of open-loop trajectory prediction. If this was the only aircraft moving on the surface, open-loop prediction would be reasonable. In reality however, aircraft moving on the surface interact with each other as the arrivals taxi-in towards their gates and departures taxi-out towards the runways. Aircraft have to stop at intersections to let other aircraft pass. Similarly, they have to often stop and wait for the active runway to be clear prior to crossing it. Separation rules also have to be followed. Departures also have to queue and wait prior to entering the runway so that there is adequate separation with respect to the prior aircraft that took off from the same runway. These rules have been programmed in the Surface Operation Simulator and Scheduler (SOSS) that is being developed at NASA Ames Research Center. SOSS uses kinematic models of different types of aircraft and the node-link graph to simulate surface traffic. While SOSS has been designed to work with schedulers for optimizing surface operations, SOSS has been used without a scheduler in this study. Routes from gate to runway, gate departure times and aircraft types are input to SOSS to simulate surface traffic for generating the results discussed in the section below.

IV. Results

The SOSS-model-based method, described in Section III, and a data-driven method are evaluated. The first method consists of using SOSS. This means that ramp-area, movement-area and queue-area speeds specified for each aircraft type are used in the prediction. The second method is a data-driven method in which average taxi-times derived from several days of actual data are added to the gate-out time or the spot crossing time for predictions.

Nineteen hours, 5:00 am to 12:00 midnight, of each day of Dallas-Fort Worth surface traffic data derived from 8/8/2011 to 8/13/2011 SDSS logs were processed to create inputs for the two methods and for validating the predictions. These days had good weather. There were a total of 5,208 arrivals and 5,256 departures. Table 10 lists

the number of arrivals and departures, and the flow configuration on each day. DFW is operated in the south-flow configuration 70% of the time.[3] On the 11th, DFW switched from south-flow configuration to north-flow configuration at 2:00 p.m. local time and then back to south-flow configuration at 5:00 p.m. DFW switched from north-flow configuration to south-flow configuration at 8:30 a.m. on the 13th.

Table 10. Selected days.

Date	# Arrivals	# Departures	Day	Flow
8/8/2011	868	881	Monday	South
8/9/2011	870	860	Tuesday	South
8/10/2011	900	902	Wednesday	South
8/11/2011	897	915	Thursday	South, North, South
8/12/2011	888	892	Friday	South
8/13/2011	785	806	Saturday	North, South

The SOSS-based method and the data-driven method were used to generate estimates of queue-area entry time, runway entry time, wheels-off time, queue-area entry sequence and runway entry sequence. These times and sequences were compared against actual values derived from SDSS logs. Queue-area entry, runway entry and wheels-off time are defined using Fig. 6 as an example. Figure 6 shows the locations of queue-area entry nodes, hold nodes and departure nodes related to runway 17R. Observe that the queue-area entry nodes are placed such that the queue is set up in the correct order. For example, an aircraft on taxiway J could enter the queue-area earlier if the entry-node were placed closer to the intersection of taxiways J and Y than an aircraft that enters upstream on taxiway J (near the queue-entry node on taxiway J depicted in the figure) and still be behind the upstream aircraft. To maintain the correct order of entry into the queue, the queue-entry node is placed at the last entry node along the taxiway in the queue-area. In SOSS simulation, aircraft movement is simulated from gate to spot, from spot to runway hold node, from hold node to departure node and from departure node to wheels-off. For the example in Fig. 6, queues are formed along taxiways EF, EG and EH and taxiways J, K and L as aircraft wait to reach the runway hold nodes. SOSS computes spot crossing time, runway hold node arrival time, wait time at the hold node, departure node arrival time, wait time at the departure node and wheels-off time. Time from departure node to wheels-off is specified for different types of aircraft. Queue-entry time is determined as the time when SOSS simulated aircraft position is at or just prior to the queue-area entry node. Runway entry time is determined by adding the wait time at the hold node to the hold node arrival time. Actual hold node arrival time, runway entry time and wheels-off time are obtained by processing the track data obtained from SDSS logs with airport geometry data. Results obtained using the two methods are discussed below.

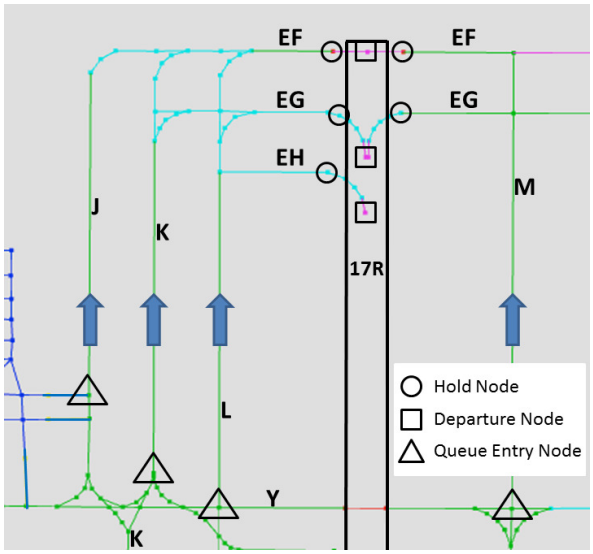

Figure 6. Examples of queue-area entry nodes, hold nodes and departure nodes.

SOSS-Model-Based

Figure 7 shows the histogram of the difference between the actual queue-area entrance time of the departures and the estimated queue-area entry times derived from SOSS simulation of 19 hours of 8/11/2011 Dallas-Fort Worth surface traffic consisting of 897 arrivals and 915 departures. August 11 was challenging because of airport configuration change from south-flow to north-flow and then back to south-flow. During the south-flow to north-flow change, departures for 35L left their gates and queued in the queue-area and waited for a long time for departures and arrivals in the previous south-flow configuration to clear the runways. Queue-area entry time results shown in Fig. 7 were computed with respect to spot crossing time. This means that the SOSS simulation used spot position and time as initial conditions. The histogram in Fig. 7 shows the maximum error to be 21 minutes. It was determined that about 80% of the actual departures arrived within two-minutes early to one-minute window with respect to SOSS-based prediction of queue-area entry time. The two-minutes early to one-minute late window is

used as the wheels-off time requirement in Ref. 12 for Precision Departure Capability for Call For Release. Later on results are presented with respect to gate departure time. Gate-based results were found to be worse than the spot-based results.

Figure 8 shows the cumulative absolute estimation error. For example, absolute value of queue-area entry time error is less than two-minutes for 87% and less than five-minutes for 97% of the departures. The main source of queue-area entry time error is the aircraft speeds assumed in SOSS. Actual maximum speeds in SDSS logs were found to be much higher in several instances compared to the nominal speeds assumed for the aircraft type in SOSS. The maximum speed difference was found to be 16 knots compared to SOSS speed of 15 knots. Average difference was found to be 8 knots for August 11 data. These findings suggest that SOSS nominal speeds can be better tuned to improve the estimates.

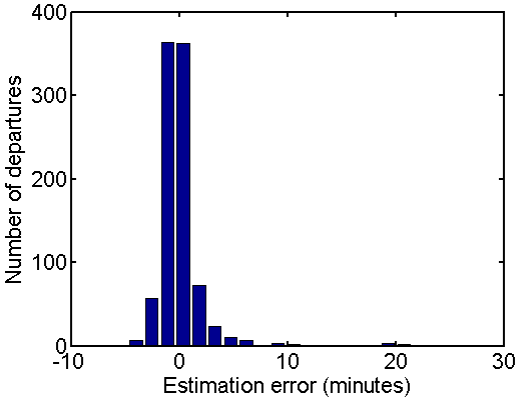

Figure 7. Queue-area entry time estimation error.

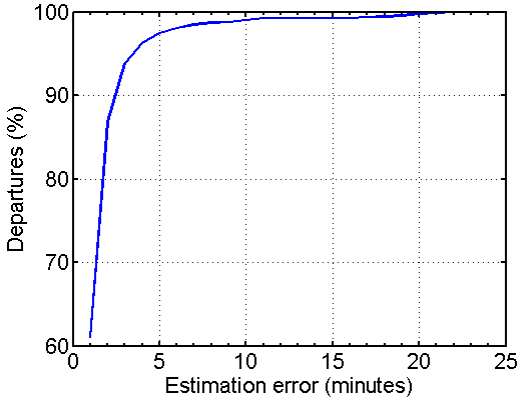

Figure 8. Cumulative absolute value of the queue-area entry time estimation error.

Figure 9 shows the histogram of the difference between the actual wheels-off time of the flights and the estimated wheels-off time derived from SOSS simulation with reference to spot crossing. Maximum wheels-off time error was found to be 24 minutes. 47% of the departures were within the two-minutes early to one-minute late window and 59% were within the plus-minus two-minute window. 86% were within the plus-minus five-minute window. The cumulative absolute wheels-off time estimation error is given in Fig. 10. Comparing Fig. 9 to Fig. 7 and Fig. 10 to Fig. 8, it may be seen that queue-area entry time estimation is much better than wheels-off time estimation. Part of the reason is that Dallas-Fort Worth has multiple queues in the queuing-area from which flights exit to enter the runway. Currently a simple logic of first-in first-out based on the queue-area entry time is being used to determine runway entry order. In the real operations, flights that need to comply with traffic flow management initiatives are given priority. Better prediction of runway entry time, which directly affects wheels-off time prediction, might require knowledge of flight priority.

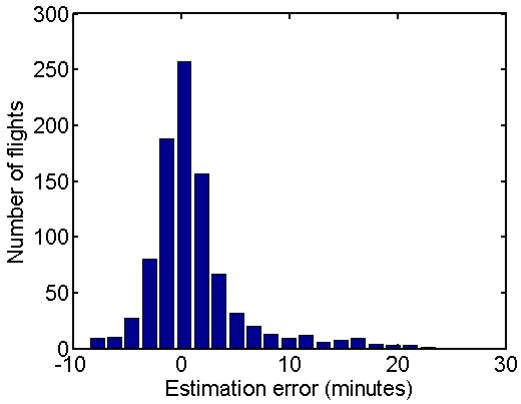

Figure 9. Wheels-off time estimation error.

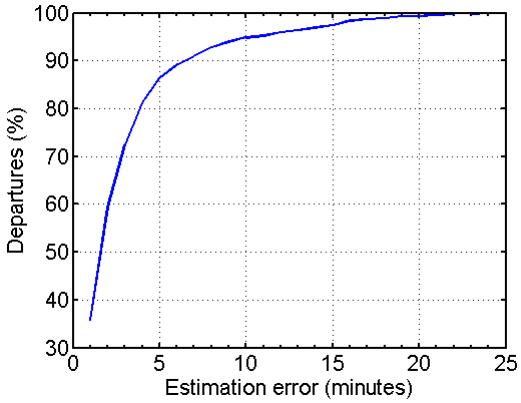

Figure 10. Cumulative absolute value of wheels-off time estimation error.

Queue-area entry time, runway entry time and wheels-off time estimation errors were computed with spot and gate as references for the six days listed in Table 10. The two-minute early to one-minute late compliance results are summarized in Table 11.

Table 11. Compliance within two-minutes early to one-minute late.

Date	Spot-based			Gate-based		
	Queue (%)	Runway (%)	Wheels-off (%)	Queue (%)	Runway (%)	Wheels-off (%)
8	85.8	64.0	58.2	60.0	47.1	46.3
9	83.7	53.7	50.3	63.3	44.5	40.9
10	84.7	58.5	53.3	61.0	47.0	44.9
11	80.1	52.6	47.0	59.5	42.4	38.6
12	87.3	58.0	51.8	63.0	49.0	46.1
13	84.6	60.4	54.2	62.4	51.4	47.5

The next set of results is for queue-area entry and runway entry sequences. To determine queue-area entry sequence for SOSS simulated aircraft and actual aircraft (based on SDSS track data), time of arrival at the queue entry nodes are sorted in increasing order for departures going to each runway. Sequence error is then computed as the difference between the actual aircraft and SOSS simulated aircraft positions in the sorted lists. This same procedure is repeated to determine runway entry sequence error. It should be noted that the runway entry sequence is same as the wheels-off sequence because only one aircraft is permitted to be on an active runway at a time. Table 12 shows the percentages of departures without sequence errors on the six days. Table 13 shows percentages with at most one sequence error. This means that the actual aircraft was either in the correct sequence or was just ahead or just behind the SOSS predicted sequence. These results show that sequence errors are reduced when spot crossing time is used as a reference for SOSS-based predictions. Maximum spot-based queue-area and runway entry

Table 12. No sequence error.

Date	Spot-based		Gate-based	
	Queue (%)	Runway (%)	Queue (%)	Runway (%)
8	70.4	62.0	49.5	47.1
9	65.9	51.7	52.7	44.4
10	72.9	59.1	48.8	45.0
11	69.1	54.8	51.4	45.2
12	72.2	62.6	53.6	47.9
13	72.5	64.5	52.0	48.3

Table 13. At most one sequence error.

Date	Spot-based		Gate-based	
	Queue (%)	Runway (%)	Queue (%)	Runway (%)
8	94.6	90.7	85.9	83.2
9	93.3	83.5	85.5	77.2
10	94.6	90.7	84.1	81.2
11	93.0	86.3	85.9	80.0
12	92.9	89.0	84.9	81.4
13	95.2	91.4	85.0	81.8

sequence errors were found to be 13 and 12, respectively, on August 8 data. The highest gate-based queue-area and runway entry sequence errors were found to be 12 and 12, respectively, also on August 8 data.

Results for the six days show that there is a significant loss of estimation accuracy from queue-area entry to runway entry. The loss is less from runway entry to wheels-off. Gate-based results are worse than spot-based results because of imprecise gate-out time information. Gate-out time is estimated based on the proximity of the SDSS reported position to the gate and SDSS reported speed, which indicates movement.

SDSS-Based Average Taxi-Time

This method assumes that historical taxi-time data from spot and gate to queue-area entry locations and wheels-off are available. This method like the SOSS-based method, discussed in the previous section, does not assume that surface surveillance information is available in real-time. Historical information can be derived from the Out-Off-On-In (OOOI) data provided by airlines and Automatic Dependent Surveillance (ADS) position reports provided by ADS equipped aircraft. To compute the spot and gate to queue-area and wheels-off taxi-times, six days of surface data were processed to identify the unique 226 spot-runway and 522 gate-runway combinations. Next, the number of departures associated with spot-runway and gate-runway were counted. Analysis showed that 25% of the spot-runway combinations were used by a single aircraft, 36% were used by two or fewer aircraft and 61% were used by 10 or fewer aircraft. The maximum number of times the spot-runway combination was used was 301 times. Of the 522 gate-runway combinations, 31% were used by only one departure, 45% were used by two or fewer departures and 57% were used by 10 or fewer departures. The maximum number of times was 38. The six days of taxi-time data were averaged and assigned to each spot-runway and gate-runway pair. Queue-entry and wheels-off times were predicted by adding the spot crossing time or the gate departure time to the average taxi-times. The actual queue-entry time and wheels-off time of the departures were compared to these predictions.

Table 14. Compliance within two-minutes early to one-minute late.

Date	Spot-based		Gate-based	
	Queue (%)	Wheels-off (%)	Queue (%)	Wheels-off (%)
8	86.9	56.5	77.7	50.6
9	86.2	50.0	77.7	48.1
10	86.6	52.5	78.4	51.6
11	81.7	54.6	74.5	52.1
12	86.8	53.3	77.2	50.9
13	86.1	57.4	77.8	55.6

Table 14 shows the percentages of departures that could be predicted within the two-minutes early to one-minute late compliance window. This table also shows that spot-based estimates are a bit better than gate-based estimates. Comparing the gate-based results in Table 11 to those in Table 14, it is seen that both queue-area entry time and wheels-off time errors are less with this method. One of the reasons for better results is that the average taxi-time is same as the actual taxi-time in instances of single departures associated with a spot-runway or gate-runway pair. The second reason is that the taxi-times based on actual track data include the influence of the actual path (not the idealized node-link path) and speed. The maximum queue-entry time and wheels-off time errors were 29 minutes and 26 minutes on August 8, respectively, when spot crossing time was used as the reference for estimation. Wheels-off time could be predicted within plus-minus five-minutes for at least 90% of the departures. This minimum value of 90% was obtained for August 11 data. Maximum queue-entry time error of 27 minutes and wheels-off time error of 24 minutes were obtained with gate-based predictions of August 8 departures. At a minimum, wheels-off time of 89% percent of departures in each of the six days could be predicted within plus-minus five-minutes. The percentage, 89%, was lowest for August 11 departures. August 13 gate-based wheels-off result of 55.6% in Table 14 are close to 59.2% obtained with the neural network in Ref. 3. Wheels-off time compliance of 53.5% of neural network predictions with respect to six days, August 7 through 12, of training data is comparable to the average compliance of 51.5% in Table 14.

Queue-area entry and runway entry sequence error results are given in Tables 15 and 16. Maximum queue-area entry and runway entry sequence errors were obtained with August 8 data. For spot-based estimates, these were 14 and 12 departures. For gate-based estimates, these errors were 11 and 10. The sequence errors for each of the six days were found to be very close to those obtained with the method described in the previous section. Comparing the results in Tables 15 and 16 to Tables 12 and 13, it is seen that the gate-based estimates are a bit better with the SDSS-based Average Taxi-time model compared to with the SOSS-based simulation method. These results suggest that the Average Taxi-Time model could be used for predictions at all airports without resorting to a more detailed simulation based approach. This method is also simple to implement, it does not require airport geometry and the

node-link models if gate departure time based wheels-off time and runway entry sequence predictions are desired. Gate-out and wheels-off data reported by airlines can be used to determine the average gate to wheels-off taxi-time needed by this model. The method is also computationally efficient because an addition operation is required for estimating wheels-off time and sorting is required to estimate the runway entry sequence.

Table 15. No sequence error.

Date	Spot-based		Gate-based	
	Queue (%)	Runway (%)	Queue (%)	Runway (%)
8	71.7	64.9	63.1	52.4
9	70.0	54.2	60.0	51.0
10	71.7	58.4	61.5	50.8
11	68.3	52.2	63.0	47.3
12	74.6	60.4	59.4	52.7
13	73.4	58.6	61.8	51.9

Table 16. At most one sequence error.

Date	Spot-based		Gate-based	
	Queue (%)	Runway (%)	Queue (%)	Runway (%)
8	96.0	91.4	90.3	87.1
9	93.4	84.5	88.3	81.5
10	95.6	90.6	91.9	85.5
11	93.9	83.2	90.7	81.1
12	94.1	89.5	90.5	86.9
13	95.4	89.7	90.2	86.0

V. Conclusions and Future Work

In the first part of this paper, 29 airports were identified for development and testing of wheels-off estimation methods after removing airports with Airport Surface Detection Equipment Model-X (ASDE-X), small-hub airports and non-hub airports from the set of 77 major U. S. airports tracked in the Federal Aviation Administration's Aviation System Performance Metrics database. These 29 airports were classified into three groups using a K-Means procedure based on taxi-out delay, traffic management delay counts and number of commercial operations. Within these three groups, San Jose International, Cleveland-Hopkins International and San Francisco International are recommended for further development and validation of wheels-off time estimation methods. San Jose has the least number of commercial operations and San Francisco has the most. In the second part of the paper, a simulation based method and a data-driven method, which uses historical taxi-time information, for estimating queue-area entry time, runway entry time and wheels-off time were described. Queue-area entry time, runway entry time and wheels-off time estimates were generated with reference to spot crossing time and gate departure time for six days of August 2011 Dallas-Fort Worth surface traffic data. These estimates were compared with the actual values determined by processing actual ASDE-X based aircraft position data. The main findings are as follows. Spot-based estimates are better compared to gate-based estimates. The data-driven method produces better gate-based estimates compared to the Surface Operation Simulator and Scheduler (SOSS) based method assuming model speeds. If surface surveillance data are unavailable, the data-driven method could be used for estimating queue-area entry time, runway entry time and wheels-off time. This method could also be used for estimating queue-area and runway entry sequence. These conclusions are expected to be equally applicable to airports such as San Jose, Cleveland and San Francisco. The next step consists of creating a geometry and node-link model for the San Jose airport with the data received from the City of San Jose. Several days of San Jose airport surface surveillance data acquired via the Low Cost Ground Surveillance (LCGS) system will be processed to create the parameters and inputs needed by the data-driven model and by the SOSS-based simulation. The estimates generated by these methods will then be compared with LCGS derived values.

References

[1]Mosaic ATM, Inc., "Airport Surface Traffic Management Requirements Resulting from Variations in Airport Characteristics: Report on Airport Survey," NASA Contract Number: NNA12AA14C, Mosaic ATM, Inc., 801 Sycolin Road, SE, Suite 306, Leesburg, VA 20175-5686, March 21, 2012.

[2]Jung, Y., Hoang, T., Montoya, J., Gupta, G., Malik, W., Tobias, L., and Wang, H., "Performance Evaluation of a Surface Traffic Management Tool for Dallas/Fort Worth International Airport," *9th USA/Europe Air Traffic Management Research and Development Seminar*, 2011, pp. 1–10.

[3]Chatterji, G. B., and Zheng, Y., "Wheels-Off Time Prediction Using Surface Traffic Metrics," AIAA-2012-5699, *Proceedings of 12th AIAA Aviation Technology, Integration, and Operations (ATIO) Conference*, Indianapolis, Indiana, Sep. 17-19, 2012.

[4] Federal Aviation Administration, URL: http://www.faa.gov/airports/planning_capacity/passenger_allcargo_stats/passenger/ [cited: 2/25/2013].

[5]Appendix A of the Mediation to Finality process adopted by the Federal Aviation Administration and the National Air Traffic Controllers Association, "Air Traffic Control Complexity Formula for Terminal and En Route Pay Setting by Facility," May 12, 2009, URL: http://nwp.natca.net/Documents/Arbitration_Award.pdf [cited: 2/25/2013].

[6]Federal Aviation Administration, "Terminal Area Forecast Summary Fiscal Years 2011-2040," URL: http://www.faa.gov/about/office_org/headquarters_offices/apl/aviation_forecasts/taf_reports/media/TAF_summary_report_FY20112040.pdf [cited: 2/25/2013].

[7]Federal Aviation Administration Air Traffic Organization, "Annual Runway Safety Report 2010," URL: http://www.faa.gov/airports/runway_safety/news/publications/media/Annual_Runway_Safety_Report_2010.pdf [cited: 2/25/2013].

[8]Federal Aviation Administration, "Low Cost Ground Surveillance (LCGS)," URL: http://www.faa.gov/about/office_org/headquarters_offices/ang/offices/ac_td/td/projects/lcgs/ [cited: 2/25/2013].

[9]Federal Aviation Administration, "NextGen Implementation Plan," March 2012, URL: http://www.faa.gov/nextgen/implementation/media/NextGen_Implementation_Plan_2012.pdf [cited: 2/25/2013].

[10]Chatterji, G. B., and Musaffar, B., "Characterization of Days Based on Analysis of National Airspace System Performance Metrics," AIAA-2007-6449, *Proceedings of AIAA Guidance, Navigation and Control Conference and Exhibit*, Hilton Head, South Carolina, Aug. 20-23, 2007.

[11]Lee, H., and Romer, T. F., "Automating the Process of Terminal Area Node-Link Model Generation," AIAA 2008-7101, *Proc. AIAA Modeling and Simulation Technologies Conference and Exhibit*, Honolulu, Hawaii, August 18-21, 2008.

[12]Capps A., and Engelland, S. A., "Characterization of Tactical Departure Scheduling in the National Airspace System," AIAA 2011-6835, *Proc. AIAA Aviation Technology, Integration and Operations Conference (ATIO)*, Virginia Beach, VA, September 20-22, 2011.

Acknowledgements

The authors thank Dr. Tatsuya Kotegawa, Dr. Waqar Malik, William Chan and Dr. Banavar Sridhar for their careful review and suggestions for improving the paper.

Appendix

The 77 major U. S. airports in the ASPM database are listed in Table. A-1. Table A-2 lists the numerical values of the eight metrics analyzed in the paper.

Table A-1. 77 ASPM airports.

#	Airport Code	Airport Name	Location
1	ABQ	Albuquerque International Sunport	Albuquerque, New Mexico
2	ANC	Ted Stevens Anchorage International	Anchorage, Alaska
3	ATL	Hartsfield - Jackson Atlanta International	Atlanta, Georgia
4	AUS	Austin-Bergstrom International	Austin, Texas
5	BDL	Bradley International	Windsor Locks, Connecticut
6	BHM	Birmingham-Shuttlesworth International	Birmingham, Alabama
7	BNA	Nashville International	Nashville, Tennessee
8	BOS	General Edward Lawrence Logan International	Boston, Massachusetts
9	BUF	Buffalo Niagara International	Buffalo, New York
10	BUR	Bob Hope	Burbank, California
11	BWI	Baltimore/Washington International Thurgood Marshall	Baltimore, Maryland
12	CLE	Cleveland-Hopkins International	Cleveland, Ohio
13	CLT	Charlotte/Douglas International	Charlotte, North Carolina
14	CVG	Cincinnati/Northern Kentucky International	Covington, Kentucky
15	DAL	Dallas Love Field	Dallas, Texas
16	DAY	James M Cox Dayton International	Dayton, Ohio
17	DCA	Ronald Reagan Washington National	Washington, District of Columbia
18	DEN	Denver International	Denver, Colorado
19	DFW	Dallas/Fort Worth International	Dallas-Fort Worth, Texas
20	DTW	Detroit Metropolitan Wayne County	Detroit, Michigan
21	EWR	Newark Liberty International	Newark, New Jersey
22	FLL	Fort Lauderdale/Hollywood International	Fort Lauderdale, Florida
23	GYY	Gary/Chicago International	Gary, Indiana
24	HNL	Honolulu International	Honolulu, Hawaii
25	HOU	William P Hobby	Houston, Texas
26	HPN	Westchester County	White Plains, New York
27	IAD	Washington Dulles International	Washington, District of Columbia
28	IAH	George Bush Intercontinental/Houston	Houston, Texas
29	IND	Indianapolis International	Indianapolis, Indiana
30	ISP	Long Island Mac Arthur	New York, New York
31	JAX	Jacksonville International	Jacksonville, Florida
32	JFK	John F Kennedy International	New York, New York
33	LAS	Mc Carran International	Las Vegas, Nevada
34	LAX	Los Angeles International	Los Angeles, California
35	LGA	La Guardia	New York, New York
36	LGB	Long Beach (Daugherty Field)	Long Beach, California
36	MCI	Kansas City International	Kansas City, Missouri
38	MCO	Orlando International	Orlando, Florida
39	MDW	Chicago Midway International	Chicago, Illinois
40	MEM	Memphis International	Memphis, Tennessee
41	MHT	Manchester	Manchester, New Hampshire
42	MIA	Miami International	Miami, Florida
43	MKE	General Mitchell International	Milwaukee, Wisconsin
44	MSP	Minneapolis-St Paul International/Wold-Chamberlain	Minneapolis, Minnesota

Table A-1. 77 ASPM airports (Contd.).

#	Airport Code	Airport Name	Location
45	MSY	Louis Armstrong New Orleans International	New Orleans, Louisiana
46	OAK	Metropolitan Oakland International	Oakland, California
47	OGG	Kahului	Kahului, Hawaii
48	OMA	Eppley Airfield	Omaha, Nebraska
49	ONT	Ontario International	Ontario, California
50	ORD	Chicago O'Hare International	Chicago, Illinois
51	OXR	Oxnard	Oxnard, California
52	PBI	Palm Beach International	West Palm Beach, Florida
53	PDX	Portland International	Portland, Oregon
54	PHL	Philadelphia International	Philadelphia, Pennsylvania
55	PHX	Phoenix Sky Harbor International	Phoenix, Arizona
56	PIT	Pittsburgh International	Pittsburgh, Pennsylvania
57	PSP	Palm Springs International	Palm Springs, California
58	PVD	Theodore Francis Green State	Providence, Rhode Island
59	RDU	Raleigh-Durham International	Raleigh/Durham, North Carolina
60	RFD	Chicago/Rockford International	Chicago/Rockford, Illinois
61	RSW	Southwest Florida International	Fort Myers, Florida
62	SAN	San Diego International	San Diego, California
63	SAT	San Antonio International	San Antonio, Texas
64	SDF	Louisville International -Standiford Field	Louisville, Kentucky
65	SEA	Seattle-Tacoma International	Seattle, Washington
66	SFO	San Francisco International	San Francisco, California
67	SJC	Norman Y. Mineta San Jose International	San Jose, California
68	SJU	Luis Munoz Marin International	San Juan, Puerto Rico
69	SLC	Salt Lake City International	Salt Lake City, Utah
70	SMF	Sacramento International	Sacramento, California
71	SNA	John Wayne-Orange County	Santa Ana, California
72	STL	Lambert-St Louis International	St Louis, Missouri
73	SWF	Stewart International	Newburgh, New York
74	TEB	Teterboro	Teterboro, New Jersey
75	TPA	Tampa International	Tampa, Florida
76	TUS	Tucson International	Tucson, Arizona
77	VNY	Van Nuys	Van Nuys, California

Table A-2. Airport metrics.

#	Airport Code	Avg. Taxi-out Delay (min.)	Avg. Taxi-out Delay Ratio (%)	TMI-from Delay Counts	Itinerant Air-carrier and Air-taxi Ops.	TMI-to Weather Delay Counts	TMI-to Volume Delay Counts	Enplanements	Level
1	ABQ	2.51	23.9	293	99,799	0	0	2,768,435	9
2	ANC	1.66	14.0	132	186,698	9	2	2,354,987	8
3	ATL	7.52	37.0	11,132	916,824	5,561	1,271	44,414,121	12
4	AUS	1.97	17.3	858	113,111	0	0	4,436,661	9
5	BDL	2.67	20.8	1,229	86,838	0	0	2,772,315	7
6	BHM	2.34	19.8	363	58,694	0	0	1,429,282	8
7	BNA	2.43	21.1	1,576	142,247	2	0	4,673,047	9
8	BOS	5.2	28.7	5,734	355,607	8,964	80	14,180,730	10
9	BUF	2.38	19.7	1,764	80,645	0	0	2,582,597	8
10	BUR	2.07	18.9	412	67,726	0	0	2,144,915	7
11	BWI	3.35	26.7	4,715	258,540	561	97	11,067,319	9
12	CLE	2.74	21.9	2,203	179,382	146	11	4,401,033	10
13	CLT	5.52	30.9	4,308	513,802	1,468	1,558	19,022,535	12
14	CVG	1.93	13.9	2,531	157,367	20	1	3,422,466	11
15	DAL	1.78	19.2	458	116,414	300	173	3,852,886	8
16	DAY	2.57	19.8	821	48,217	0	0	1,247,333	8
17	DCA	4.3	26.7	7,565	278,757	895	95	9,053,004	10
18	DEN	3.71	26.5	3,302	630,969	1,702	7	25,667,499	12
19	DFW	3.26	22.7	5,296	640,541	1,592	5	27,518,358	12
20	DTW	3.25	18.5	4,149	436,534	997	303	15,716,865	11
21	EWR	8.49	40.4	6,476	402,988	26,201	1,419	16,814,092	10
22	FLL	4.16	26.2	4,397	227,061	25	20	11,332,466	9
23	GYY	0.09	0.8	10	1,574	0	0	1,420	0
24	HNL	1.96	15.5	29	206,446	0	0	8,689,699	11
25	HOU	1.8	19.9	593	139,280	112	238	4,753,554	8
26	HPN	2.39	18.8	1,946	64,601	59	171	972,385	7
27	IAD	4.04	25.2	5,766	314,384	899	350	11,044,383	11
28	IAH	4.84	29.3	4,031	516,708	797	166	19,306,660	12
29	IND	2.02	16.6	1,886	141,111	49	0	3,670,396	9
30	ISP	1.51	17.5	136	19,828	0	0	781,396	7
31	JAX	2.22	18.0	1,191	77,315	0	0	2,700,514	9
32	JFK	8.5	32.7	9,296	405,976	8,896	975	23,664,832	10
33	LAS	3.79	26.6	2,700	484,194	416	131	19,872,617	11
34	LAX	3.96	26.6	4,503	583,167	808	321	30,528,737	11
35	LGA	11.67	47.3	10,716	364,140	19,845	3,195	11,989,227	10
36	LGB	2.23	16.7	297	36,839	0	0	1,512,212	8
36	MCI	2.21	19.6	1,603	136,398	0	0	5,011,000	9
38	MCO	3.67	27.3	3,831	300,075	95	29	17,250,415	11
39	MDW	2.99	27.1	1,855	209,789	661	42	9,134,576	8
40	MEM	2.14	14.1	1,883	291,700	550	11	4,344,213	10
41	MHT	2.03	18.2	1,145	51,376	0	0	1,342,308	5
42	MIA	3.43	21.2	2,623	375,209	247	122	18,342,158	12

Table A-2. Airport metrics (Contd.).

#	Airport Code	Avg. Taxi-out Delay (min.)	Avg. Taxi-out Delay Ratio (%)	TMI-from Delay Counts	Itinerant Air-carrier and Air-taxi Ops.	TMI-to Weather Delay Counts	TMI-to Volume Delay Counts	Enplanements	Level
43	MKE	2.8	22.0	1,911	157,302	36	1	4,671,976	9
44	MSP	3.72	22.5	3,441	418,739	1,341	8	15,895,653	11
45	MSY	2.1	19.9	905	103,304	0	0	4,255,411	9
46	OAK	1.82	19.8	339	131,981	2	1	4,550,526	8
47	OGG	1.46	17.0	10	100,155	0	0	2,683,933	7
48	OMA	2.21	18.9	625	78,769	0	0	2,047,055	6
49	ONT	2.14	22.0	283	74,575	0	0	2,271,458	6
50	ORD	5.6	33.8	13,077	871,099	25,195	249	31,892,301	12
51	OXR	1.86	20.9	4	3,634	0	0	3	0
52	PBI	2.35	18.6	1,573	79,399	0	1	2,877,158	9
53	PDX	2.3	20.0	887	190,108	0	0	6,808,486	8
54	PHL	6.56	33.8	9,960	433,307	13,653	1,726	14,883,180	12
55	PHX	3.77	27.2	2,471	438,901	250	249	19,750,306	11
56	PIT	2.9	21.8	2,284	127,723	6	0	4,070,614	10
57	PSP	2.64	22.2	412	30,175	0	0	759,510	7
58	PVD	2.44	20.3	1,920	57,194	0	0	1,920,699	8
59	RDU	3.2	23.4	3,557	144,399	23	0	4,462,508	9
60	RFD	0.1	0.9	27	12,208	0	0	102,559	7
61	RSW	2.42	20.0	1,172	74,321	0	0	3,748,366	8
62	SAN	3.17	24.5	1,959	174,034	111	16	8,465,683	7
63	SAT	2.63	23.4	845	115,339	18	0	3,992,304	10
64	SDF	1.58	13.3	1,263	136,804	48	9	1,650,707	9
65	SEA	2.58	18.3	1,646	311,087	4	0	15,971,676	9
66	SFO	4.4	26.8	1,848	386,941	18,679	24	20,056,568	9
67	SJC	1.83	17.9	347	106,557	0	0	4,108,006	7
68	SJU	1.96	14.8	193	136,249	0	0	3,983,130	7
69	SLC	4.54	26.1	1,159	284,537	18	5	9,701,756	10
70	SMF	2.19	21.2	457	101,800	3	0	4,370,895	6
71	SNA	3.36	28.7	1,046	91,715	1	0	4,247,802	9
72	STL	1.95	18.2	1,935	179,075	9	0	6,159,090	9
73	SWF	1.3	9.9	195	13,215	0	0	209,966	0
74	TEB	0.11	1.0	5,260	60,600	305	260	5,071	7
75	TPA	2.42	20.3	1,628	166,407	41	8	8,174,194	11
76	TUS	2.58	23.3	296	57,648	0	0	1,779,679	8
77	VNY	0.12	1.1	134	10,687	3	0	1,018	8